PHYSICAL REVIEW A **79**, 030301(R) (2009)

Hyperentanglement of two photons in three degrees of freedom

Giuseppe Vallone,[1,2,3,*] Raino Ceccarelli,[2,*] Francesco De Martini,[2,3,4,*] and Paolo Mataloni[2,3,*]
[1]*Centro di Studi e Ricerche "Enrico Fermi," Via Panisperna 89/A, Compendio del Viminale, Roma 00184, Italy*
[2]*Dipartimento di Fisica della Sapienza Università di Roma, Roma 00185, Italy*
[3]*Consorzio Nazionale Interuniversitario per le Scienze Fisiche della Materia, Roma 00185, Italy*
[4]*Accademia Nazionale dei Lincei, via della Lungara 10, Roma 00165, Italy*
(Received 24 October 2008; published 9 March 2009)

A six-qubit hyperentangled state has been realized by entangling two photons in three degrees of freedom. These correspond to the polarization, the longitudinal momentum, and the indistinguishable emission produced by a two-crystal system operating with type I phase matching in the spontaneous parametric down conversion regime. The state has been characterized by a chained interferometric apparatus and its complete entangled nature has been tested by a witness criterion specifically presented for hyperentangled states. The experiment represents a realization of a genuine hyperentangled state with the maximum entanglement between the two particles allowed in the given $2^3 \times 2^3$ Hilbert space.

DOI: 10.1103/PhysRevA.79.030301 PACS number(s): 03.67.Bg, 42.50.Dv, 42.65.Lm

Hyperentangled (HE) two-photon states, i.e., quantum states of two photons simultaneously entangled in N independent degrees of freedom (DOFs) [1,2], are nowadays recognized as a basic resource for many quantum information (QI) processes. At variance with n-photon entanglement, hyperentanglement is much less affected by decoherence. Moreover, the detection efficiency of the state, which scales as η^n (η is the quantum efficiency of detectors), is not reduced by growing the size of the state.

Two-photon HE states have been used to demonstrate the enhancement of the channel capacity in superdense coding [3], the complete analysis of the four orthogonal polarization Bell states [4,5], and for the engineering of efficient four-qubit two-photon cluster states [6], successfully used in the realization of basic quantum computation (QC) algorithms in the one-way model [7–9]. Finally, advanced tests of quantum nonlocality enabling to enhance the violation of local realism are possible when operating in a large-dimension Hilbert space with two-photon N-DOF HE states [10–12]. Increasing the number N of DOFs necessarily implies an exponential growing of resources. Nevertheless, according to the current technology, for $N=2$, 3, or 4 this approach is still convenient in terms of decoherence, repetition rate, and detection-generation efficiency than increasing the number of entangled particles. Hence, we can conceive in a medium term perspective a *hybrid* approach to multiqubit entanglement based on the simultaneous entanglement of more than one photon pair in $N=2$, 3, and 4 DOFs.

HE states of increasing size are of paramount importance for the realization of even more challenging objectives. In the framework of the one-way QC, using a six-qubit cluster state, a controlled-NOT (CNOT) gate operating over the entire Bloch sphere of the target and control qubits and other important quantum algorithms such as the extension of the Deutsch-Josza algorithm [13] can be realized. Recently, optical schemes involving two or more photons and expanding the available Hilbert space to incredibly large dimensions were realized. In particular three DOFs, namely, polarization, spatial mode, and time-energy, were used to build a multidimension entangled state of two photons encoded in four qubits and two qutrits [14]. More recently, Greenberger-Horne-Zeilinger states of up to ten qubits were engineered by exploiting polarization and momentum of five photons [15]. It is worth noting that in both experiments the addition of one DOF, i.e., time-energy and linear momentum, respectively, derives from a local manipulation[1] of polarization entanglement without increasing the entanglement between the particles. Indeed, in both experiments the additional DOF entanglement was not independent from polarization entanglement[2].

A "genuine" HE state, given by the product of N Bell states [16], one for each DOF,

$$|\Psi_N\rangle = |\mathrm{Bell}_1\rangle \otimes |\mathrm{Bell}_2\rangle \otimes \cdots \otimes |\mathrm{Bell}_N\rangle, \tag{1}$$

allows us to enlarge the available Hilbert space. Let us consider the *entropy of entanglement* of the state $|\Psi_N\rangle$,

$$E(|\Psi_N\rangle) = S[\mathrm{tr}_A(|\Psi_N\rangle\langle\Psi_N|)] = S[\mathrm{tr}_B(|\Psi_N\rangle\langle\Psi_N|)], \tag{2}$$

where S is the standard von Neumann entropy defined as $S(\rho)=\mathrm{tr}(\rho \log_2 \rho)$. It is easy to demonstrate in this case that $E(|\Psi\rangle)=N$, independently of any local operation. Hence the state $|\Psi_N\rangle$ has the maximum allowed entanglement for a given number N.

We have engineered and characterized a six-qubit HE state based on the simultaneous triple entanglement of two photons. By our scheme two polarization (π) entangled pho-

*http://quantumoptics.phys.uniroma1.it/

[1]We define local manipulation as any transformation that acts separately on each particle.

[2]In Ref. [14] experiment a Franson-type polarization interferometer, realized for each photon by a quartz birefringent element, was used for the analysis of time-energy entanglement. Polarization and time-energy entanglement become "independent" and the total available entanglement can increase if two standard Franson interferometers are used [18].

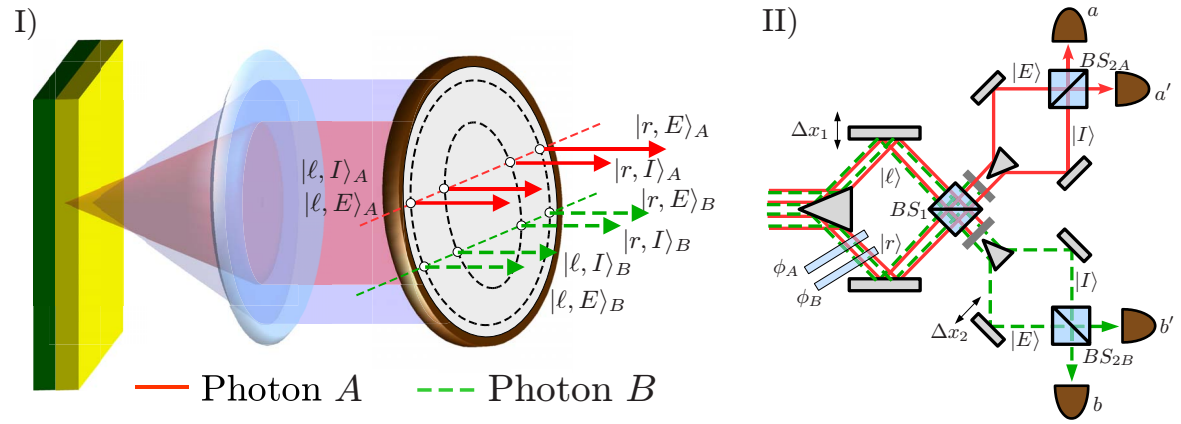

FIG. 1. (Color online) Experimental setup. (I) The two-crystal system generates photon pairs with equal probability over the internal (I) and external (E) cones. Polarization entanglement arises from double passage of the pump beam through the crystals and the combined action of a spherical mirror and a $\lambda/4$ wave plate (not shown in the figure). The annular sections of each emission cone, with diameters d_I=12 mm and d_E=16 mm are intercepted by a single eight-hole screen. (II) Measurement setup: the first interferometer [ending with $(BS)_1$] measures momentum entanglement in the basis $\frac{1}{\sqrt{2}}(|\ell\rangle+e^{i\phi_{A,B}}|r\rangle)$ at the same time for Alice (red line) and Bob (dotted green line) photons. Phases ϕ_A (ϕ_B) are set by tilting a thin glass plate intercepting the Alice (Bob) mode. The subsequent interferometers, corresponding to $(BS)_{2A}$ and $(BS)_{2B}$, perform the measurement separately for the Alice and Bob photons in the basis $\frac{1}{\sqrt{2}}(|I\rangle\pm|E\rangle)$. The interference filters allowing photon detection within a bandwidth $\Delta\lambda$=6 nm and the four apparatus for polarization analysis aligned before each detector are not shown in the figure.

tons experience a further double entanglement in the longitudinal momentum DOF. This was done by selecting four pairs of correlated **k** modes within the *double-cone* emission of a two-crystal system operating in the spontaneous parametric down conversion (SPDC) regime. This configuration realizes a genuine HE state of two photons entangled in N=3 independent DOFs, labeled as π, **k**, and **c**. Note that linear momentum DOF is naturally entangled in the SPDC process. However, so far, no experiments were designed to use other DOFs besides one polarization and one linear momentum to create entanglement. In the present experiment we realized a source and a measurement device allowing manipulation and measurement of a triple entanglement (i.e., polarization+two linear momenta) by selecting four pairs of SPDC modes. Indeed, we do not increase the entanglement of the SPDC process, but the entanglement of the state that we are able to measure and manipulate.

The system used to generate the six-qubit HE state consisted of two 0.5-mm-thick type I β barium borate (BBO) crystal slabs, cut at different phase matching angles and aligned one behind the other [see Fig. 1(I)]. They were operating under double excitation (back and forth) of a vertically (V) polarized continuous wave (cw) laser at wavelength (wl) λ_p. The polarization entangled Bell state $|\Phi^-\rangle=\frac{1}{\sqrt{2}}(|H\rangle_A|H\rangle_B-|V\rangle_A|V\rangle_B)$ was created by spatial superposing the two perpendicularly polarized emission cones of each type I crystal [2].

Photon pairs were created with equal probability at degenerate wl $\lambda=2\lambda_p$ by either one of BBO crystals along two correlated directions belonging to the lateral surfaces of two cones, with full aperture angles θ_I=4.6° and θ_E=6.1°, respectively. We refer to them as the "internal" (I) and the "external" (E) cone, corresponding to the first and the second crystals, respectively. The two "photon choices" corresponding to the I and E cones are thus identified as a third independent DOF. Coherence and hence indistinguishability between the two crystal emissions were guaranteed by the coherence length of the pump, exceeding by more than 1 order of magnitude the total crystal length. Double longitudinal momentum entanglement was created by selecting four pairs of correlated modes with a eight-hole screen. Precisely, the following correlated mode pairs $|I,\ell\rangle_A$-$|I,r\rangle_B$ and $|I,r\rangle_A$-$|I,\ell\rangle_B$ were selected for the first crystal and $|E,\ell\rangle_A$-$|E,r\rangle_B$ and $|E,r\rangle_A$-$|E,\ell\rangle_B$ for the second crystal emission. It is worth to remember that only two photons, namely, A (Alice) and B (Bob), are generated with equal probability by either one of the crystals. We label the corresponding mode emission as ℓ (r) by referring to the left (right) side of each cone and as I (E) by considering the internal (external) cone [see Fig. 1(I)].

The produced state, expressed as a six-qubit HE state, is given by the product of one polarization entangled state and two longitudinal momentum entangled states, i.e.,

$$\frac{1}{\sqrt{2}}(|H\rangle_A|H\rangle_B+e^{i\varphi_\pi}|V\rangle_A|V\rangle_B)\otimes\frac{1}{\sqrt{2}}(|\ell\rangle_A|r\rangle_B+e^{i\varphi_{\mathbf{k}}}|r\rangle_A|\ell\rangle_B)$$

$$\otimes\frac{1}{\sqrt{2}}(|I\rangle_A|I\rangle_B+e^{i\varphi_{\mathbf{c}}}|E\rangle_A|E\rangle_B). \quad (3)$$

In the case of a pure state the entropy of entanglement equals the number N=3 of DOFs. It corresponds to the maximum entanglement between the two particles in a $2^3\times2^3$ Hilbert space, as said.

The measurement setup used to test the triple entanglement is given by the chained interferometric apparatus sketched in Fig. 1(II). It is composed of two parts. The first one performs the measurement of the momentum entanglement existing within each emission cone. Here the ℓ modes are spatially and temporally matched with the r modes both

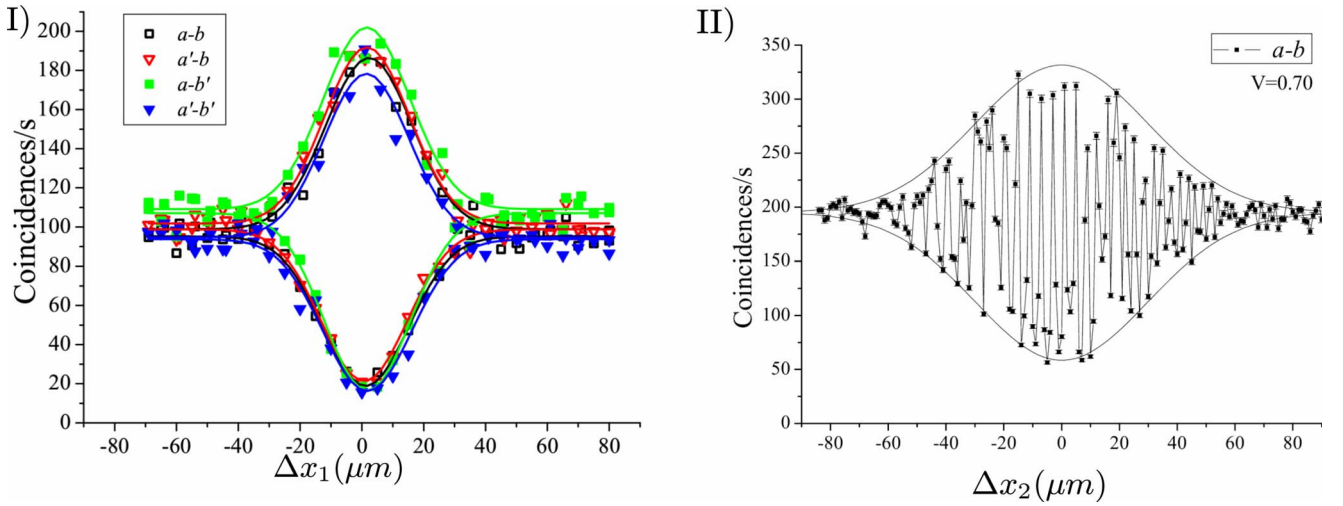

FIG. 2. (Color online) (I) Coincidence rates $a-b$, $a'-b$, $a-b'$, and $a'-b'$ vs Δx_1 for state (3) showing the typical dip ($\varphi_{\mathbf{k}}=0$)-peak ($\varphi_{\mathbf{k}}=\pi$) feature with average visibility $V=0.815\pm0.027$ (dip) and $V=0.877\pm0.017$ (peak). The corresponding experimental fits are also shown. Full width at half maximum (FWHM) $\simeq$30 nm of the interference patterns is in agreement with the expected value for a filter bandwidth of 6 nm. (II) Coincidence rate $a-b$ vs Δx_2 for state (3) with $\varphi_{\mathbf{k}}=\pi$ with visibility $V\simeq0.70$ and FWHM $\simeq$60 nm. In both cases the time average of each experimental point is 3*s*.

for the up (*A* photon) and down (*B* photon) sides of a common 50:50 beam splitter $[(\mathrm{BS})_1]$, for the *I* and *E* emission cones. In the second part of the apparatus, measuring momentum entanglement between the two crystal emissions, the left (right) $(\mathrm{BS})_1$ output modes belonging to the Alice (Bob) photon are then injected into another interferometer where the *I* and *E* modes are matched onto the $(\mathrm{BS})_{2A}$ $[(\mathrm{BS})_{2B}]$ beam splitter. Two trombone mirror assemblies mounted on motorized translation stages enable fine adjustment of path delays Δx_1 and Δx_2 between the different mode sets in the first and second parts of the interferometric apparatus. Phase setting of **k** momentum entanglement is achieved by careful tilting of thin glass plates ϕ_A and ϕ_B, placed, respectively, on the Alice and Bob right modes [cf. Fig. 1(II)]. Four single-photon detectors, model Perkin Elmer SPCM-AQR14, detect the radiation belonging to the Alice output modes of $(\mathrm{BS})_{2A}$, namely, *a* and *a*′ in Fig. 1(II), and to the Bob output modes of $(\mathrm{BS})_{2B}$ [*b* and *b*′ in Fig. 1(II)]. Polarization entanglement is measured by using four standard polarization analyzers, one for each detector.

The experimental results given in Fig. 2(I) show the characteristic interference patterns obtained by measuring the coincidences $a-b$, $a-b'$, $a'-b$, and $a'-b'$ as a function of Δx_1. Momentum entanglement is demonstrated by the typical dip-peak transition obtained by adjusting the state phase. In the same way, similar interference traces were obtained for the four sets of coincidences by varying Δx_2 in the second interferometer. We show in Fig. 2(II) the one corresponding to the measurement of $a-b$ coincidences. We observe the different effects on phase stability appearing in the figures: in the first interferometer ($|\ell\rangle$-$|r\rangle$ measurement) the phase $\varphi_{\mathbf{k}}$ is self-stabilized since any mirror instability corresponds to a global phase variation of the state. Moreover, since any change in Δx_1 determines the simultaneous variation of all the $|r\rangle$ mode optical delays, even in this case the phase remains constant. This feature is evident in Fig. 2(I), where we show the different coincidence patterns for $\varphi_{\mathbf{k}}=0$ and $\varphi_{\mathbf{k}}=\pi$.

In the second interferometer ($|I\rangle$-$|E\rangle$ measurement) the phase $\varphi_{\mathbf{c}}$ is not self-stabilized and a compact interferometer is needed to improve the phase stability. Moreover, the variation of Δx_2 changes only the $|E\rangle$ path delay of the *B* photon. This corresponds in Fig. 2(II) to a random $\varphi_{\mathbf{c}}$ phase variation. For the same reason the FWHM duration of the interference pattern of Fig. 2(II) doubles the one of Fig. 2(I). The complexity of the measurement setup, where spatial matching of different modes is performed onto the two BS sets, is the main reason of experimental imperfections that lower the visibility values and hence the purity of the HE state. The adoption of a waveguide integrated measurement setup [17] instead of using a bulk interferometric apparatus would allow in a near future to largely improve the measured visibilities.

The entanglement existing in the generated HE state was detected by using a criterion recently proposed for hyperentanglement [16]. It is based on the evaluation of some witnesses specifically presented for graph states. For each DOF spanning a two-dimensional Hilbert space, we associate the states $|H\rangle$, $|\ell\rangle$, and $|I\rangle$ to the basis vector $|0\rangle$, while $|V\rangle$, $|r\rangle$, and $|E\rangle$ are associated to $|1\rangle$. By setting all the phases φ_μ (with $\mu=\pi$, **k**, and **c**) to zero, the following HE state is obtained:

$$|\Psi_3\rangle=|\phi^+\rangle_\pi\otimes|\psi^+\rangle_{\mathbf{k}}\otimes|\phi^+\rangle_{\mathbf{c}} \tag{4}$$

with the standard Bell states $|\phi^+\rangle=\frac{1}{\sqrt{2}}(|0\rangle_A|0\rangle_B+|0\rangle_A|0\rangle_B)$ and $|\psi^+\rangle=\frac{1}{\sqrt{2}}(|0\rangle_A|1\rangle_B+|1\rangle_A|0\rangle_B)$. We also define Z_i, z_i, and z_i' ($i=A,B$) as the σ_z Pauli matrices for the π, **k**, and **c** DOFs, respectively. Similarly, X_i, x_i, and x_i' represent the corresponding σ_x matrices.

The presence of entanglement between the two photons for each separate DOF was first verified by tracing the other DOFs and evaluating separately an entanglement witness for π, **k**, and **c** entanglement using the following witnesses:

$$W_\pi = (\mathbb{1}_\pi - 2X_A X_B - 2Z_A Z_B) \otimes \mathbb{1}_{\mathbf{k}} \otimes \mathbb{1}_{\mathbf{c}}, \tag{5a}$$

$$W_{\mathbf{k}} = \mathbb{1}_\pi \otimes (\mathbb{1}_{\mathbf{k}} - 2x_A x_B + 2z_A z_B) \otimes \mathbb{1}_{\mathbf{c}}, \tag{5b}$$

$$W_{\mathbf{c}} = \mathbb{1}_\pi \otimes \mathbb{1}_{\mathbf{k}} \otimes (\mathbb{1}_{\mathbf{c}} - 2x'_A x'_B - 2z'_A z'_B). \tag{5c}$$

The negative experimental values $W_\pi = -0.6298 \pm 0.0080$, $W_{\mathbf{k}} = -0.7987 \pm 0.0055$, and $W_{\mathbf{c}} = -0.4101 \pm 0.0082$ demonstrate the entanglement in each DOF.

As explained in [16], these measurement are not sufficient to ensure that the prepared state is a genuine HE state. Indeed states with negative values of W_π, $W_{\mathbf{k}}$, and $W_{\mathbf{c}}$ do exist that can be prepared by a classical mixture of several simple entangled (i.e., entangled in only one DOF) states. We then need to measure a witness able to detect the global entanglement of the HE state. It has been demonstrated [16] that the following operators can be used in our case:

$$W_2 = 3 - 2\left(\prod_{k=1}^{3} \frac{S_{2k}+1}{2} + \prod_{k=1}^{3} \frac{S_{2k-1}+1}{2}\right),$$

$$W_3 = 2 - 3\prod_{k=1}^{3}\left(\frac{1 + S_{2k-1} + S_{2k}}{3}\right), \tag{6}$$

where $S_1 = X_A X_B$, $S_2 = Z_A Z_B$, $S_3 = x_A x_B$, $S_4 = -z_A z_B$, $S_5 = x'_A x'_B$, and $S_6 = z'_A z'_B$ are the *stabilizers* of the hyperentangled state (4). The expectation value of both the witnesses is equal to -1 for a pure triple HE state. The experimental values of the witnesses, $W_2 = -0.1182 \pm 0.0055$ and $W_3 = -0.0890 \pm 0.0037$, obtained by the measured operators given in Table I, demonstrate that the produced state cannot be obtained by a classical mixture of states that are separable in one or more DOFs and thus represents a genuine HE state.

TABLE I. Experimental values of the operators needed to measure W_π, $W_{\mathbf{c}}$, $W_{\mathbf{k}}$, W_2, and W_3.

S_1	S_2	S_3	S_4
0.733 ± 0.006	0.897 ± 0.005	0.810 ± 0.005	0.989 ± 0.002
S_5	S_6	$S_1 S_3$	$S_1 S_5$
0.420 ± 0.008	0.990 ± 0.002	0.681 ± 0.007	0.443 ± 0.008
$S_3 S_5$	$S_1 S_3 S_5$	$S_2 S_4 S_6$	$S_2 S_4$
0.398 ± 0.008	0.445 ± 0.008	0.891 ± 0.005	0.893 ± 0.005
$S_2 S_6$	$S_4 S_6$		
0.895 ± 0.005	0.988 ± 0.002		

In this Rapid Communication we have presented an optical scheme enabling the simultaneous entanglement of two photons in three independent DOFs, corresponding to the polarization and two different longitudinal momenta derived by the indistinguishable emission of two nonlinear crystals. The entanglement of the state was tested by using an entanglement witness method specifically presented for HE states. Our results represent a realization of a two-photon six-qubit HE state with three independently entangled DOFs. The number of **k** modes involved in type I emission processes can be very large; hence, HE states with even larger size are expected by the technique described in this Rapid Communication, but at the price of a large number of **k** modes in which the photons can be detected. Other DOFs, such as energy-time [18,19] or orbital angular momentum [20], can be exploited to create larger multidimensional entangled states of two photons for novel advanced QI tasks.

We thank A. Cabello for useful discussions.

[1] P. G. Kwiat, J. Mod. Opt. **44**, 2173 (1997).
[2] M. Barbieri, C. Cinelli, P. Mataloni, and F. De Martini, Phys. Rev. A **72**, 052110 (2005).
[3] J. T. Barreiro, T.-C. Wei, and P. G. Kwiat, Nat. Phys. **4**, 282 (2008).
[4] C. Schuck, G. Huber, C. Kurtsiefer, and H. Weinfurter, Phys. Rev. Lett. **96**, 190501 (2006).
[5] M. Barbieri, G. Vallone, P. Mataloni, and F. De Martini, Phys. Rev. A **75**, 042317 (2007).
[6] G. Vallone, E. Pomarico, P. Mataloni, F. De Martini, and V. Berardi, Phys. Rev. Lett. **98**, 180502 (2007).
[7] H. J. Briegel and R. Raussendorf, Phys. Rev. Lett. **86**, 910 (2001).
[8] K. Chen *et al.*, Phys. Rev. Lett. **99**, 120503 (2007).
[9] G. Vallone, E. Pomarico, F. De Martini, and P. Mataloni, Phys. Rev. Lett. **100**, 160502 (2008).
[10] D. Collins, N. Gisin, N. Linden, S. Massar, and S. Popescu, Phys. Rev. Lett. **88**, 040404 (2002).
[11] M. Barbieri, F. De Martini, P. Mataloni, G. Vallone, and A. Cabello, Phys. Rev. Lett. **97**, 140407 (2006).
[12] A. Cabello, Phys. Rev. Lett. **97**, 140406 (2006).
[13] E. Brainis *et al.*, Phys. Rev. Lett. **90**, 157902 (2003).
[14] J. T. Barreiro, N. K. Langford, N. A. Peters, and P. G. Kwiat, Phys. Rev. Lett. **95**, 260501 (2005).
[15] W.-B. Gao *et al.*, e-print arXiv:0809.4277.
[16] G. Vallone, R. Ceccarelli, F. De Martini, and P. Mataloni, Phys. Rev. A **78**, 062305 (2008).
[17] A. Politi, M. J. Cryan, J. G. Rarity, S. Yu, and J. L. O'Brien, Science **320**, 646 (2008).
[18] J. D. Franson, Phys. Rev. Lett. **62**, 2205 (1989).
[19] A. Rossi, G. Vallone, F. De Martini, and P. Mataloni, Phys. Rev. A **78**, 012345 (2008).
[20] E. Nagali *et al.*, e-print arXiv:0810.2417.